
Title: The impact of urban morphology on the building energy consumption and solar energy generation potential of university dormitory blocks

Highlights:

- Established an analytic workflow for energy use and solar potential at block-scale
- Evaluated the impact of urban morphology on energy use and solar potential
- H-shaped block saved 12.25% EUI with the highest energy-saving potential
- Tower block reduced energy use by 72.05% after the deployment of PV panels
- Proposed multiple regression models for predicting energy performance by morphology

Abstract:

Urban morphology is a major factor affecting building energy consumption and solar potential in the urban block. The aim of this research was to evaluate the impact of urban morphology on both building energy consumption and solar energy generation potential for university dormitory blocks in Wuhan. This paper proposed a classification method for dormitory blocks, calculated the building energy consumption and solar energy generation potential of 55 blocks, and analyzed the correlation between urban morphology and three energy performance indicators: Energy Use Intensity (EUI), Solar Energy Generation Intensity (SEGI) and Net Energy Use Intensity (NEUI). Multiple regression models were used to predict energy performance by urban morphological parameters. The results indicate that different block types could lead to up to 12.25% difference in EUI, and 35.85% significant difference in building NEUI with the deployment of photovoltaic (PV) panels. The EUI is mainly affected by three

morphological parameters, which are Average length of block, Shape factor and Building density; while the SEGI and NEUI are mainly affected by Average height of block, Shape factor and Sky view factor. This study could serve as guidelines for planners and policymakers in campus planning and architectural design to improve building energy conservation at block-scale.

Keywords:

Urban morphology, Block typology, Dormitory block, Energy use intensity, Solar potential, Multiple regression model

Nomenclature

<i>ADB</i>	Average depth of block	<i>NZED</i>	Nearly-zero energy district
<i>AHB</i>	Average height of block	<i>PV</i>	Photovoltaic
<i>ALB</i>	Average length of block	<i>R value</i>	Thermal resistivity
<i>BD</i>	Building density	<i>RMSE</i>	Root Mean Squared Error
<i>EUI</i>	Energy Use Intensity	<i>SEF</i>	Sky exposure factor
<i>FAR</i>	Floor area ratio	<i>SEGI</i>	Solar Energy Generation Intensity
<i>GHG</i>	Green House Gas	<i>SF</i>	Shape factor
<i>GIS</i>	Geographic Information System	<i>SHGC</i>	Solar heat gain coefficient
<i>HDR</i>	Height to depth ratio	<i>SVF</i>	Sky view factor
<i>NEUI</i>	Net Energy Use Intensity	<i>UWG</i>	Urban Weather Generator
<i>NZEC</i>	Nearly-zero energy community		

1. Introduction

The global predicaments of energy scarcity and climate change are ubiquitous

challenges confronting all nations. The cities of the world consume about 75% of its primary energy and emit 50-60% of the world's Green House Gas (GHG) (UN-Habitat, 2021). In order to achieve carbon neutrality on a larger scale through reduced energy consumption, there is increasing interest in the concept of nearly-zero energy district (NZED) (Iturriaga et al., 2021; Amaral et al., 2018) and nearly-zero energy community (NZEC) (Suh et al., 2019; Ullah et al., 2021). These approaches focus on the intermediate scale between buildings and cities. Two strategies can be employed to reduce energy consumption in order to achieve the NZED goal: The first strategy is to minimize building energy use. The second strategy involves maximizing the supply of clean energy, which can be achieved through using PV panels in urban buildings.

1.1 Review

- (1) How could energy use be minimized by optimizing urban morphology?

Research has established that different urban block types exhibit distinct energy performance characteristics (Martins et al., 2019; Quan et al., 2021; Xu et al., 2021). Scholars have employed different classification methods, such as identifying characteristic blocks, to investigate the relationship between urban morphology and building energy consumption in various climate zones. Zhang et al. (2019) identified six prototypes in a tropical high-density city in Singapore, where it was found that Courtyard and Hybrid blocks outperformed Tower and Slab blocks, while Ahmadian et al. (2021) analyzed four prototype blocks and found that tunnel-court and pavilion types provided the best and worst energy performance, respectively. Other studies have classified real urban blocks to explore energy consumption characteristics. In Seoul, Oh

et al. (2019) identified 13 block types with energy consumption varying between 11.3% and 29.1% with decrease in the U-values of the building wall insulation, while Shi et al. (2021) found that L-shaped hospital buildings had the best energy-saving potential at a rate of 3.5%. These studies provide evidence that urban topologies significantly affect building energy consumption.

To further explore the reasons for differences in energy consumption among different types of blocks, scholars have investigated the relationship between urban morphology and building energy consumption (Wang et al., 2021; Quan et al., 2021). In terms of climate zones, Leng et al. (2020) analyzed the relationship between urban morphological parameters and building heating energy consumption in cold regions in China and found that each unit increase in perimeter-to-volume ratio reduced building heating energy consumption by 6.76%. Bansal et al. (2022) investigated the relationship between building characteristics, urban form, and residential building energy use in different local climate zone contexts in Seoul, and the results exhibited that different local climate zones significantly influenced building energy consumption and impacted the effects of building characteristics on building energy use. These studies confirm that the relationship between urban morphology and building energy performance varies in different climate zones. To further improve understanding of the complex relationship between urban morphology and building energy consumption, new research tools and frameworks have been developed, such as multi-objective urban form design optimization (Liu et al., 2023) and uncertainty and sensitivity analysis (Prataviera et al., 2022) for building energy simulations. These studies offer evidence of a significant

influence of urban morphology on building energy use, which exhibits divergent patterns across various climate zones and cities. (Quan et al., 2021).

(2) How could solar energy potential be maximized by optimizing urban morphology?

The potential for exploiting solar energy resources in cities is vast (Huang et al., 2019), and scholars have studied this issue from various perspectives. Sarralde et al. (2015) used GIS and python scripts to model 4,718 urban blocks in London, and found that solar resources on building roofs and facades have great potential for further exploitation. Similarly, Lan et al. (2021) developed an imagery-based model for assessing solar potential at block-scale, contributing high accuracy to solar potential assessment studies while reducing assessment time. Chen et al. (2022) accurately evaluated the solar radiation intensity and total roof area of buildings in Shanghai, highlighting the vast potential for solar resources. The above research findings confirm the differences in solar potential due to variations in climate and urban morphology (Wang et al. 2021).

To understand the reasons for these differences in solar potential among different block types, scholars have explored the relationship between urban morphology and solar potential. Fan et al. (2022) found that different climate zones and different urban morphologies present different solar potential. Poon et al. (2020) correlated 10 major morphological parameters in blocks with the development potential of solar energy resources, finding that the Sky exposure factor (SEF) and the Sky view factor (SVF) had the strongest correlation with the radiant illuminance of roofs and facades in

buildings. Mendis et al. (2020) proposed a method using horizontally inclined PV modules integrated into solar shading devices to address the issue of disadvantageous inclination and solar heat gains in commercial office buildings in the tropical context of Colombo, Sri Lanka. The results indicated that horizontally tilted PV integrated with shading strategies on facades can generate nearly 8% more electricity compared to the traditional vertical PV facade installations. Ren et al. (2022) developed a three-dimensional geographic information method to predict dynamic rooftop solar irradiance by considering the shading effects of surrounding buildings, finding that the urban blocks' annual solar energy potential was decreased by 35.7% due to the shading effect. Research on the influence of urban morphology on solar energy generation potential has demonstrated a close link between the two, and defining their relationship can help architects and urban planners design and plan sustainable cities more effectively.

It has been previously observed that urban morphology significantly impacts on both building energy consumption and solar energy generation potential, with different characteristics (Zhang et al., 2019; Quan et al., 2021). However, few studies have been conducted on the synergistic impact of urban morphology on building energy consumption and solar energy generation potential comprehensively. Accordingly, there is a lack of research on corresponding energy conservation planning and renewable energy strategies at the block-scale. Such knowledge will play a crucial role in promoting energy efficiency and renewable energy use in buildings for urban blocks.

In particular, existing studies assessing dormitory blocks with specific urban

morphology and climates in central China are extremely limited.

1.2 Research aim and research questions

This study aims to quantitatively evaluate the impact of urban morphology on building energy consumption and solar energy generation potential of university dormitory blocks, and to determine which morphological parameters play the greatest role in regulating the Energy Use Intensity (EUI) and Solar Energy Generation Intensity (SEGI) in the Hot-summer and Cold-winter zone in China. Based on the above evaluation, this study then attempts to provide the design strategies and recommendations to carry out energy efficiency-oriented campus planning in the future. The research aim was to further develop knowledge on the following research questions:

- (1) Does the typology of university dormitory blocks have an impact on building energy consumption and solar energy generation potential, and to what extent?
- (2) Which parameters of urban morphology have the most significant influence on regulating Energy Use Intensity and Solar Energy Generation Intensity?

2. Methodology

2.1. The framework of the study

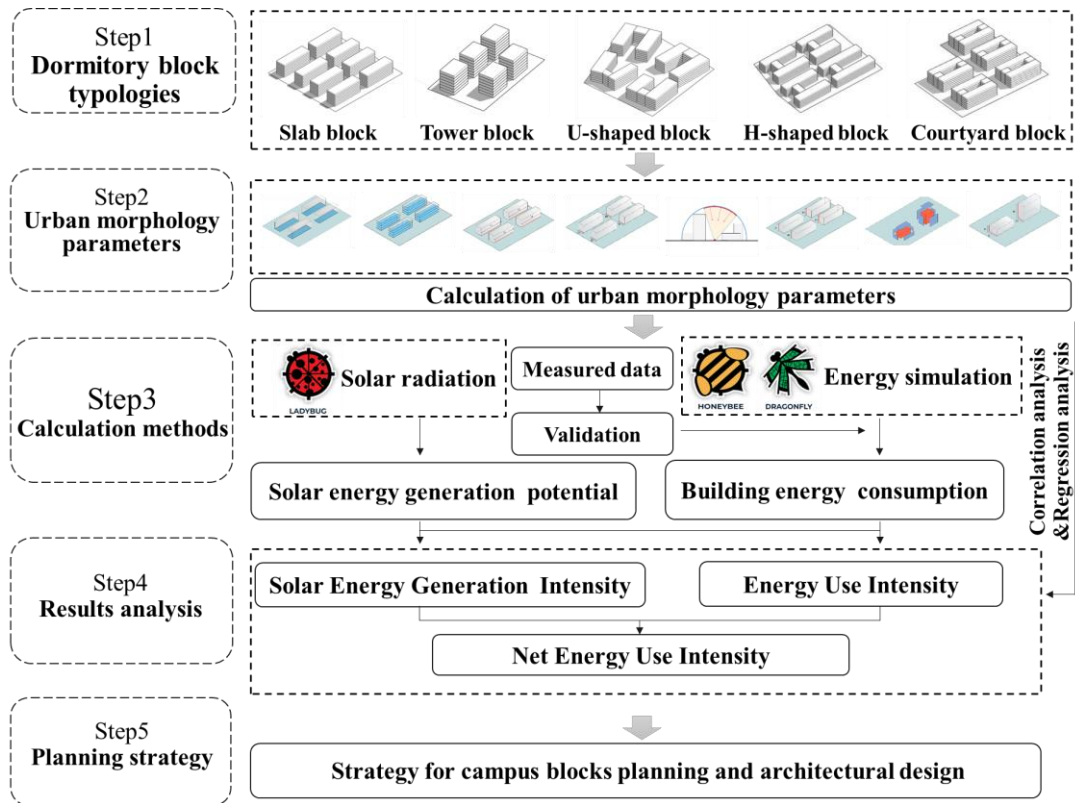


Fig. 1. Framework for evaluating impact of urban morphology on energy performance

Fig.1 illustrates a technical framework comprising five steps for evaluating the impact of urban morphology parameters on solar energy generation potential and building energy consumption.

2.2. Dormitory block typologies

2.2.1. Cases of urban blocks

Wuhan is situated at 30°52' north latitude and 114°32' east longitude in central China. The region has a north subtropical monsoon climate characterized by cold winters and hot summers. The annual sunshine hours range from 1810 to 2100, and the annual radiation ranges from 1210.56 kWh/m² to 1315.32 kWh/m² (Xu et al., 2019).

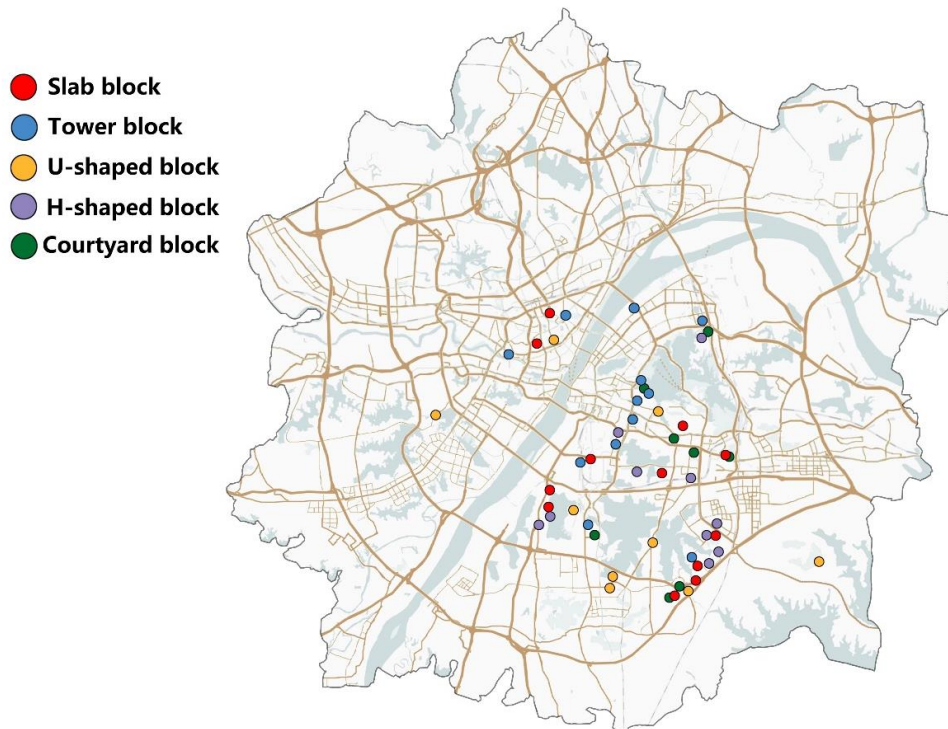


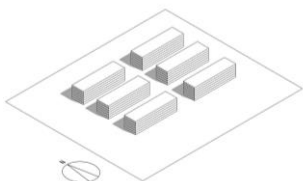

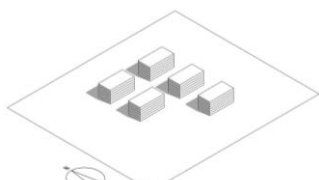

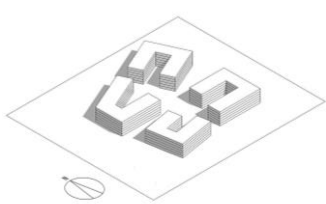
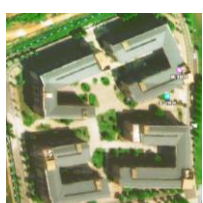
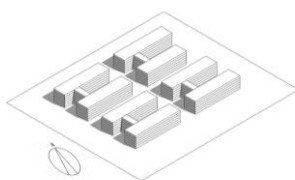
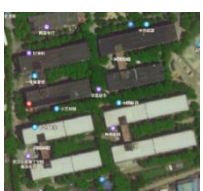
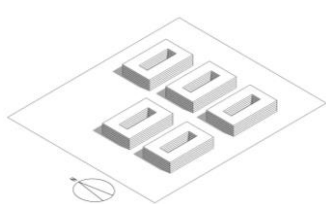

Fig.2. The distribution of 5 block types in Wuhan

Wuhan has 84 universities, each with an average of 3-4 dormitory blocks. This study focuses on a total of 55 dormitory blocks in Wuhan, which were selected from 213 existing blocks based on their size (between 100 and 300 meters in length and width) and the number of buildings (not less than 3). These dormitory blocks can be categorized into 6 types: Slab block, Tower block, U-shaped block, H-shaped block, Courtyard block, and Hybrid block. The first five types account for 84.6% of the total number of blocks, while the Hybrid blocks are mainly composed of different types of buildings, accounting for about 15.4%, which are difficult to study based on spatial form. Therefore, this study focuses on the first five types (Table 1). In view of the potential variability in building envelope and construction materials over various years of construction, this study focuses on the period spanning from the years 2000 to 2020. This timeframe is signified by a rapid expansion of higher education in Wuhan, during

which a large number of dormitory blocks were constructed to enhance the living standards of students. Accordingly, a total of 55 dormitory blocks (Fig.2) were selected from 84 universities for this research.

Table1

5 types of typical dormitory blocks

Typology	Model	Plan layout	Block features
Slab			The buildings are in the shape of a slab, and the length to width ratio of the building is greater than 2.
Tower			The buildings are approximately square shaped, and the length to width ratio of the building is less than 2.
U-shaped			The buildings are shaped like a "U", and the general U-shaped opening faces east or west.
H-shaped			The buildings are H-shaped, and the general H-shaped openings face east and west.
Courtyard			The buildings are enclosed on all sides, and there is a courtyard in the middle.

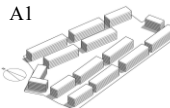
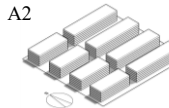
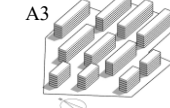
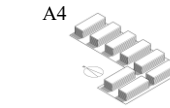
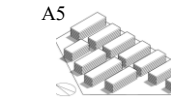
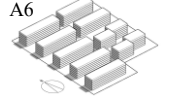
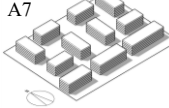
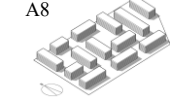
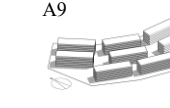
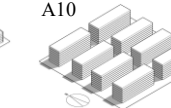
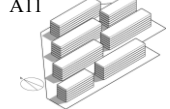
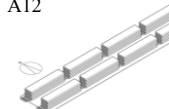
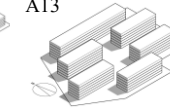

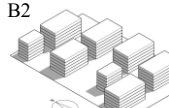

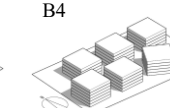
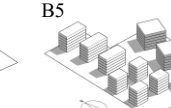
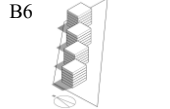
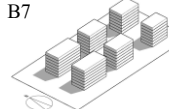
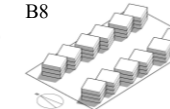
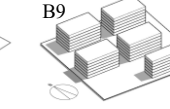
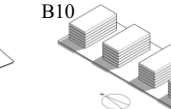
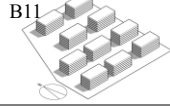
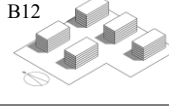
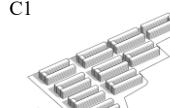
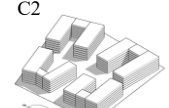
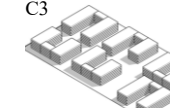
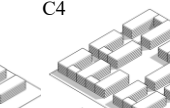
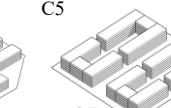
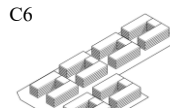
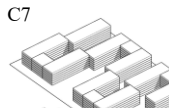

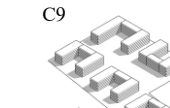
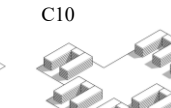
2.2.2. Acquisition of 3D model data

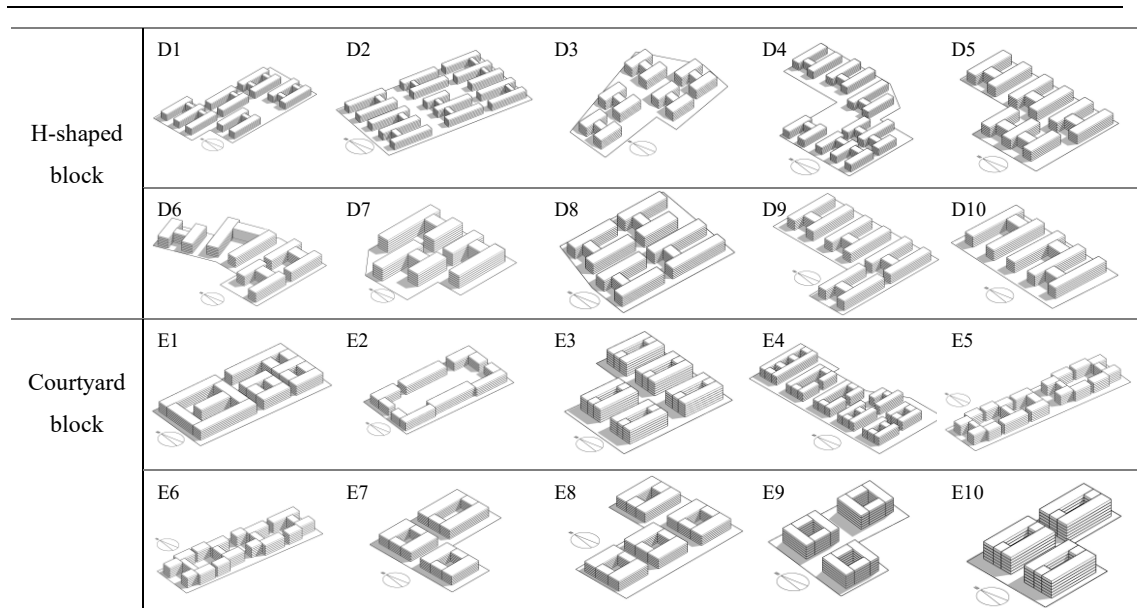
In this study, the vector data of Wuhan map were downloaded from the official

website of OpenStreetMap (OSM), and the OSM file was obtained, which contained building contour and height information. The obtained 3D model information was then calibrated according to the latest satellite maps and Baidu street view maps for building contour, layer number, and height. Finally, the corrected 3D information data was used for modeling on the Rhino platform (Table 2).

Table2

Models of 55 cases

Type	Models of Cases				
Slab block	A1 	A2 	A3 	A4 	A5 
	A6 	A7 	A8 	A9 	A10 
	A11 	A12 	A13 		
Tower block	B1 	B2 	B3 	B4 	B5 
	B6 	B7 	B8 	B9 	B10 
	B11 	B12 			
U-shaped block	C1 	C2 	C3 	C4 	C5 
	C6 	C7 	C8 	C9 	C10 



2.3. Urban morphological parameters

Urban morphology is widely used in urban studies, and can be represented in different ways with various parameters (Quan et al., 2021). When selecting the parameters for this study, it was taken into account that these parameters are generally used in urban planning practice and are easily accessible for architects, and that different types of parameters are capable of describing the spatial and layout characteristics of blocks from different perspectives. Firstly, parameters were selected that described the basic morphological characteristics of block buildings: Average length of block (ALB), Average depth of block (ADB), Average height of block (AHB) and Height to depth ratio (HDR). Secondly, the parameters that reflected the urban compactness were selected: Building density (BD), Floor area ratio (FAR) (Wang et al., 2021). Finally, the parameters that reflected the block spatial characteristics were selected: Sky view factor (SVF), Shape factor (SF).

The 8 urban morphological parameters (Table 3) have been proven to have a certain impact on building energy performance through previous studies (Quan et al.,

2021; Xu et al., 2021; Wang, et al., 2021). Based on the computational equations for the specific parameters, the results of the morphological parameters for dormitory blocks were obtained (Table 4).

Table 3

Urban morphological parameters

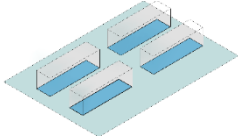
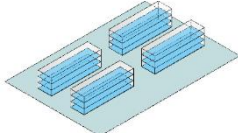
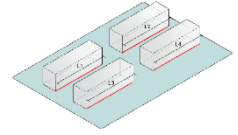
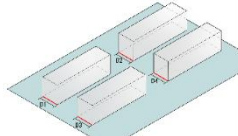
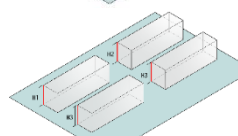
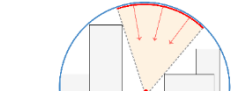
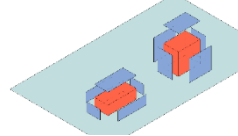
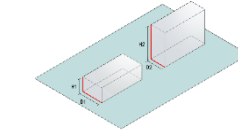
Urban morphology	Abbreviation	Computational Equation	Diagram
Building density	BD	$BD = \frac{A_D}{S_G} \times 100\%$	
Floor area ratio	FAR	$FAR = \frac{A_B}{S_G}$	
Average length of block	ALB	$ALB = \frac{\sum_{i=1}^n l_i V_i}{\sum_{i=1}^n V_B}$	
Average depth of block	ADB	$W = \frac{\sum_{i=1}^n w_i V_i}{\sum_{i=1}^n V_B}$	
Average height of block	AHB	$H = \frac{\sum_{i=1}^n h_i V_i}{\sum_{i=1}^n V_B}$	
Sky view factor	SVF	$\varphi_s = \frac{1}{\pi R^2} \int_{S_v} \cos \theta dS$	
Shape factor	SF	$SF = \frac{S_B}{V_B}$	
Height to depth ratio	HDR	$HDR = \frac{\sum_{i=1}^n ar V_i}{\sum_{i=1}^n V_B}$	

Table 4

Results of morphological parameters for dormitory blocks

Typology	Cases	ALB	ADB	AHB	SVF	SF	HDR	BD	FAR
Slab blocks	A1	67.05	17.59	18.00	51.09	0.20	1.03	0.32	1.94
	A2	75.09	22.41	18.00	35.86	0.17	0.80	0.46	2.75
	A3	50.68	10.20	18.00	57.43	0.29	1.77	0.23	1.35
	A4	66.00	22.00	18.00	50.73	0.18	0.82	0.41	2.49
	A5	58.35	19.19	18.00	59.67	0.20	0.94	0.35	2.08
	A6	50.83	15.03	18.00	50.47	0.23	1.20	0.35	2.09
	A7	46.14	19.18	18.00	56.05	0.20	0.94	0.28	1.68
	A8	56.81	18.36	18.00	56.53	0.20	0.98	0.30	1.82
	A9	56.51	15.00	18.00	55.28	0.22	1.20	0.31	1.89
	A10	59.11	18.00	24.00	45.56	0.19	1.33	0.36	2.84
	A11	63.19	15.00	18.00	54.37	0.22	1.20	0.33	1.97
	A12	80.00	15.00	18.00	46.70	0.21	1.20	0.38	2.26
	A13	62.27	15.00	18.00	51.69	0.22	1.20	0.34	2.07
Tower blocks	B1	21.19	18.49	21.00	54.25	0.23	1.14	0.29	2.03
	B2	31.42	20.87	18.00	53.36	0.21	0.88	0.31	1.87
	B3	19.81	20.87	18.00	55.36	0.24	0.86	0.29	1.74
	B4	24.90	29.49	15.00	60.12	0.20	0.51	0.32	1.61
	B5	24.41	19.02	18.00	64.84	0.25	1.04	0.21	1.26
	B6	18.71	14.94	18.00	71.41	0.30	1.20	0.18	1.10
	B7	35.45	14.16	21.00	57.35	0.25	1.49	0.23	1.62
	B8	13.00	13.00	9.00	69.25	0.42	0.69	0.31	0.92
	B9	33.53	19.06	18.00	61.96	0.22	0.97	0.28	1.69
	B10	40.00	20.00	18.00	59.95	0.21	0.90	0.34	2.04
	B11	36.00	18.00	18.00	61.26	0.22	1.00	0.24	1.42
	B12	36.00	18.00	18.00	64.49	0.22	1.00	0.21	1.27
U-shaped blocks	C1	65.39	8.93	18.00	53.29	0.32	2.02	0.27	1.60
	C2	47.18	17.10	18.00	51.67	0.22	1.07	0.38	2.27
	C3	53.83	20.75	18.00	52.65	0.20	0.91	0.36	2.13
	C4	55.00	20.86	18.00	50.56	0.19	0.89	0.39	2.34
	C5	56.08	16.09	18.00	49.07	0.22	1.12	0.42	2.52
	C6	51.64	17.58	18.00	54.91	0.21	1.03	0.36	2.15
	C7	52.24	17.89	18.00	51.76	0.21	1.01	0.43	2.60
	C8	54.05	17.48	18.00	54.31	0.21	1.06	0.37	2.24
	C9	48.67	16.22	18.00	61.97	0.22	1.14	0.27	1.61
	C10	55.30	17.39	18.00	59.11	0.21	1.05	0.29	1.75
H-shaped blocks	D1	78.42	17.45	18.00	54.04	0.20	1.05	0.36	2.15
	D2	81.92	16.03	18.00	51.69	0.21	1.15	0.33	2.00
	D3	35.37	14.46	18.00	59.13	0.26	1.26	0.30	1.83
	D4	69.17	17.51	18.00	58.36	0.20	1.03	0.53	3.21
	D5	65.27	17.97	18.00	52.12	0.20	1.00	0.41	2.44
	D6	62.12	17.17	18.00	52.35	0.21	1.06	0.40	2.42
	D7	60.80	16.19	18.00	49.27	0.22	1.11	0.40	2.38

	D8	69.37	15.94	18.00	52.60	0.22	1.14	0.38	2.30
	D9	80.68	16.04	18.00	53.55	0.21	1.12	0.36	2.14
	D10	85.57	16.26	18.00	58.04	0.21	1.11	0.35	2.12
	E1	71.59	18.06	18.00	41.47	0.20	1.00	0.53	3.16
	E2	57.42	17.39	15.00	50.13	0.23	0.88	0.36	1.79
	E3	48.24	11.65	18.00	51.69	0.28	1.55	0.39	2.34
Courtyard	E4	54.09	12.02	18.00	53.67	0.28	1.50	0.32	1.94
blocks	E5	27.95	14.45	18.00	51.41	0.27	1.27	0.37	2.20
	E6	29.99	14.34	18.00	49.75	0.27	1.28	0.40	2.39
	E7	64.32	21.41	18.00	55.30	0.19	0.87	0.44	2.62
	E8	56.29	20.92	18.00	54.38	0.20	0.88	0.43	2.59
	E9	31.72	10.65	18.00	59.39	0.31	1.69	0.32	1.93
	E10	48.24	11.65	18.00	51.94	0.28	1.55	0.44	2.63

2.4. Calculation methods

In this section, calculation methods were proposed for three energy performance indicators: EUI, SEGI and NEUI. For modeling, we selected the Rhino software and integrated the toolsets of Ladybug, Honeybee and Butterfly on the Grasshopper platform. To conduct simulations, we utilized two simulation engines: EnergyPlus for building energy simulation, and Radiance for lighting and solar radiation analysis. It is worth noting that the reliability of EnergyPlus and Radiance has been demonstrated in previous studies (Zhang et al. 2019; Wang et al. 2021).

2.4.1. The calculation method of Energy Use Intensity

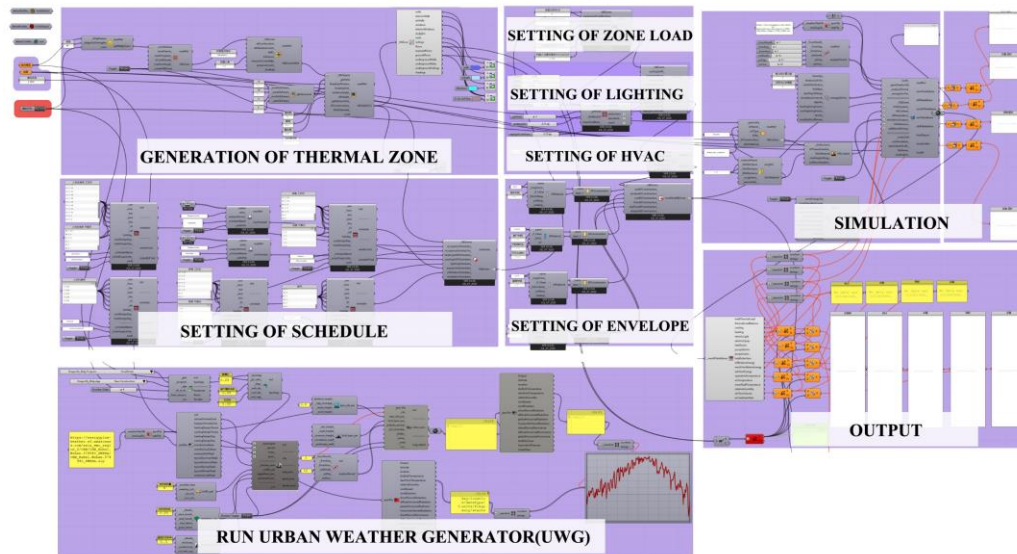


Fig.3. The simulation workflow in Grasshopper

Building energy consumption is affected by many complex factors. This study focused on the impact of urban morphology on building energy consumption. To exclude the influence of related factors other than urban morphology, the relevant simulation parameters were uniformly set through field investigation, literature and related specifications. The simulation workflow used in Grasshopper is shown in Fig.3.

According to the survey of dormitory buildings, the height of the campus dormitory model was uniformly set to 3.6 meters, the window to wall ratio of the building was set as 0.22 for the south and north facades, and 0.05 for the east and west facades. The windows were 900mm above ground level on each floor and were evenly spaced along the facade. The Wuhan epw weather data was utilised, which was downloaded from the EnergyPlus website, and represents the typical weather year at the location. The setting of the wall envelope was based on the results of field research and literature as shown in Table 5.

Table 5

Envelope structure settings for dormitory building model

Construction type	SHGC	R-Value (m ² K/W)
Roof	—	2.67
Wall	—	0.69
Ground floor	—	0.65
Window	0.284	2.295

Table 6

Parameter settings for dormitory building energy simulation

Parameter	Setting	Unit
Cooling set point	26	°C
Heating set point	18	°C
Lighting loads	5	W/m ²
Equipment loads	4	W/m ²
Occupancy	0.04	People/m ²
Air Infiltration rate	0.0003	m ³ /s • m ²
Mechanical ventilation rate	0.0002	m ³ /s • m ²

This study selected 9 representative university dormitory blocks in Wuhan to conduct field surveys and online questionnaire surveys. The total energy consumption includes four types: cooling, heating, lighting and equipment loads. The survey focused on the information of occupancy rate, energy use schedule, and heating and cooling setting temperature in order to obtain information for the cooling, heating, lighting, and equipment loads in these blocks. A total of 1216 questionnaires were collected from the survey, and according to these survey results, the parameter settings were established and then used for this study, and these are shown in Table 6.

This study measured the annual monthly electricity consumption data of a dormitory block with four buildings in Huazhong University of Science and Technology in 2019, and compared these results with the simulation results to confirm

the accuracy of the calculation model for dormitory buildings in Wuhan. The simulation input parameters for this validation were consistent with Table 5 and Table 6.

EUI is a crucial indicator in evaluating building energy consumption and is calculated by Eq. (2). EUI signifies the amount of energy used per unit of building floor area and is commonly employed in the investigation of building energy utilization, particularly in simulation research (Quan, et al., 2021; Wang et al., 2021).

$$EUI = \frac{E_T}{A_T} \quad (2)$$

EUI—Energy Use Intensity (kWh/(m²·y))

E_T—Total building energy consumption (kWh/(m²·y))

A_T—Total building floor area (m²)

2.4.2. The calculation method of Solar Energy Generation Intensity

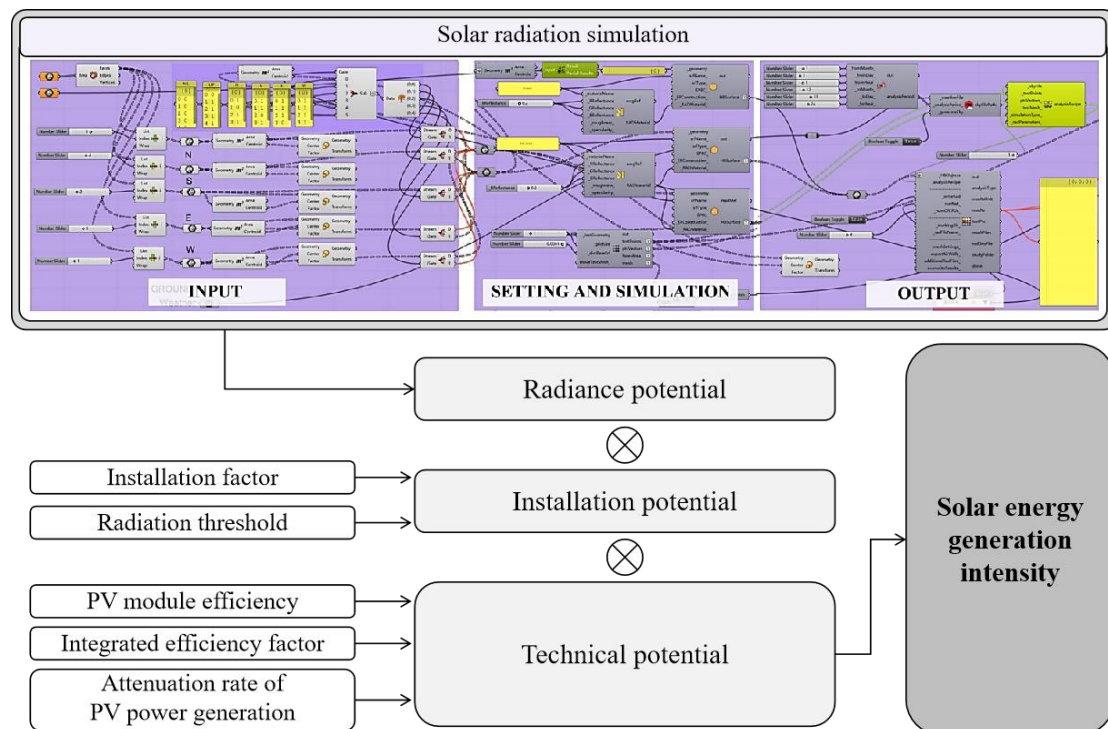


Fig.4. The simulation workflow for SEGI

This study evaluated the effect of urban morphology on the solar energy potential

generated by PV panels. However, numerous factors can influence the block-level implementation of PV panels. Izquierdo et al. (2008) proposed five levels of solar energy potential evaluation, including physical potential, geographical potential, technical potential, economic potential, and social potential. Drawing on previous research (Xu et al., 2019; Xu et al., 2021), an assessment method was developed, accounting for Wuhan's distinct climate and urban morphological characteristics. The SEGI was obtained through the block-scale solar calculation method at three levels including radiation potential, installation potential and technical potential (Fig.4).

Firstly, the radiation potential pertains to solar radiation distribution on building surfaces, determined by using the Grasshopper platform workflow with a proven high accuracy in prior studies (Liao et al., 2019; Xu et al.,2021). The installation potential is the effective area of building surfaces suitable for PV panel installation, influenced mainly by the installation factor and solar radiation threshold. The installation factor was obtained from case surveys, while the threshold value is the minimum radiation necessary to achieve PV panel break-even throughout its lifespan. When setting polycrystalline silicon PV material and a 25-year life cycle, the radiation threshold is 466 kWh/(m²·y). Lastly, the technical potential denotes the energy generation efficiency of the PV system, primarily affected by PV module efficiency, Integrated efficiency factor and Attenuation rate of PV power generation (Table 7). Other parameter settings for the solar radiation simulation are shown in Table 8.

Table 7

Setting of parameters for technical potential

Parameters settings	Value	Unit
PV module efficiency	17.87	%
Integrated efficiency factor	86	%
Attenuation rate of PV power generation	0.062	%
Durable years of PV equipment	25	year

Table 8

Setting of parameters in the simulation model

Parameters setting	Value
Weather data	CHN_Hubei.Wuhan.574940_CSWD
Simulation period	00:00 on January 1 to 24:00 on December 31
Measurement point	1 mm above the grid
Grid size	1m*1m
Building surface diffuse reflectance	0.2
Ground surface diffuse reflectance	0.2

In summary, this study calculated the annual energy production of the PV system by Eq. (3).

$$E_p = H_A \times A_{pv} \times \eta \times K \times (1 - R_d)^{N-1} \quad (3)$$

E_p —Annual energy generation of PV equipment (kWh/y)

H_A —Annual accumulated solar radiation on building surface (kWh/y)

A_{pv} —Available installation area for PV panels (m²)

η —PV module efficiency (%)

K —Integrated efficiency factor (%)

R_d —Attenuation rate of PV power generation (%)

N —Durable years of PV equipment (y)

To be consistent with the research on building energy consumption in the block, the solar energy potential was calculated based on the unit building floor area. Solar energy generation potential is expressed as Solar Energy Generation Intensity (SEGI),

which is often used to measure the solar energy potential for a building or block (Zhang et al., 2019; Xu et al., 2021). It is calculated by Eq. (4).

$$SEGI = \frac{E_S}{A_T} \quad (4)$$

SEGI—Solar Energy Generation Intensity (kWh/(m²·y))

E_S—Annual solar energy generation of PV panels (kWh/y)

A_T—Total floor area (m²)

2.4.3. The calculation method of Net Energy Use Intensity

The impact of urban morphology on both building EUI and SEGI can vary significantly. In this study, Net Energy Use Intensity (NEUI) was adopted to comprehensively evaluate the building energy consumption with PV deployment, which is a common measure utilized to reflect the intensity of energy use after the integration of renewable energy (Zhang, et al., 2019). It is calculated by subtracting solar energy generation intensity from energy use intensity of buildings in a block, and reflects the net energy consumption of buildings in a block per year after accounting for the solar energy generation potential. It is calculated according to Eq. (5).

$$NEUI = EUI - SEGI \quad (5)$$

NEUI—Net Energy Use Intensity(kWh/(m²·y))

EUI—Energy Use Intensity(kWh/(m²·y))

SEGI—Solar Energy Generation Intensity(kWh/(m²·y))

3. Results

3.1. Results of validation

Fig.5 shows the red line as the measured electricity consumption of the dormitory

block in 2019, and the blue line represents the output of the EnergyPlus simulation model. It can be seen that there was a good correlation between the measured energy consumption and the energy consumption simulated by the model. To validate the accuracy of the developed calculation model, this study employed the Root Mean Squared Error (RMSE), which produced a value of 0.45. Additionally, the coefficient of determination (R^2) was calculated, yielding a value of 0.91. These results indicate that the simulation model produced accurate results within an acceptable range.

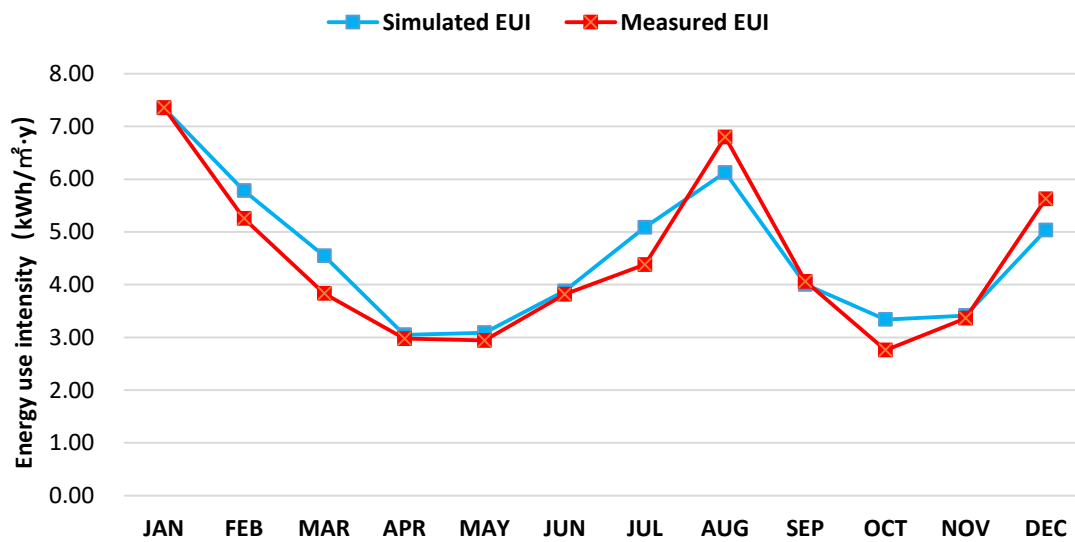


Fig.5. Comparison of simulated and measured energy consumption

3.2. Energy Use Intensity

Fig.6 displays significant variation in EUI values for heating and cooling across different case studies, while lighting and equipment EUI remained almost constant. Cooling EUI was found to be highest in the Tower block case B6 (12.46 kWh/(m²·y)), and lowest in the H-shaped block case D10 (9.19 kWh/(m²·y)) with a difference of 3.27 kWh/(m²·y), representing a percentage difference of 35.58%. The result of the standard deviation amongst the 55 blocks was 0.78 for cooling EUI, however the heating EUI

demonstrated even greater variation. The highest and lowest values for heating EUI were observed in the tower block case B8 (11.55 kWh/(m²·y)), and the H-shaped block case D10 (3.95 kWh/(m²·y)) with a difference of 7.6 kWh/(m²·y), representing a percentage difference of 192.4%. The result of standard deviation for heating EUI amongst the 55 blocks was 1.77, in contrast to that of 0.78 for the cooling EUI. Accordingly, the variance for cooling EUI over the 55 blocks was 0.88, and that for the heating EUI was 1.33. The F-Test was carried out for these results, which suggests that if the 2 variances are not significantly different, the result will be close to 1 (Bland, 2015). However, the F-test for the variances of cooling and heating EUI provided a result of 1.60, suggesting that there was a greater variation caused in heating EUI than cooling EUI due to the effects of block typology. Therefore, the large variation in percentage difference and standard deviation when comparing the cooling and heating EUI of the blocks, together with the F-test value suggested that the impact of block typology on heating EUI was greater than that on cooling EUI.

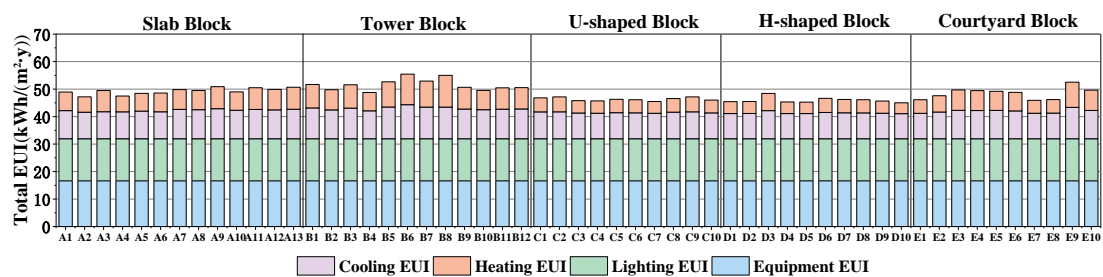


Fig.6. The total EUI of 55 blocks

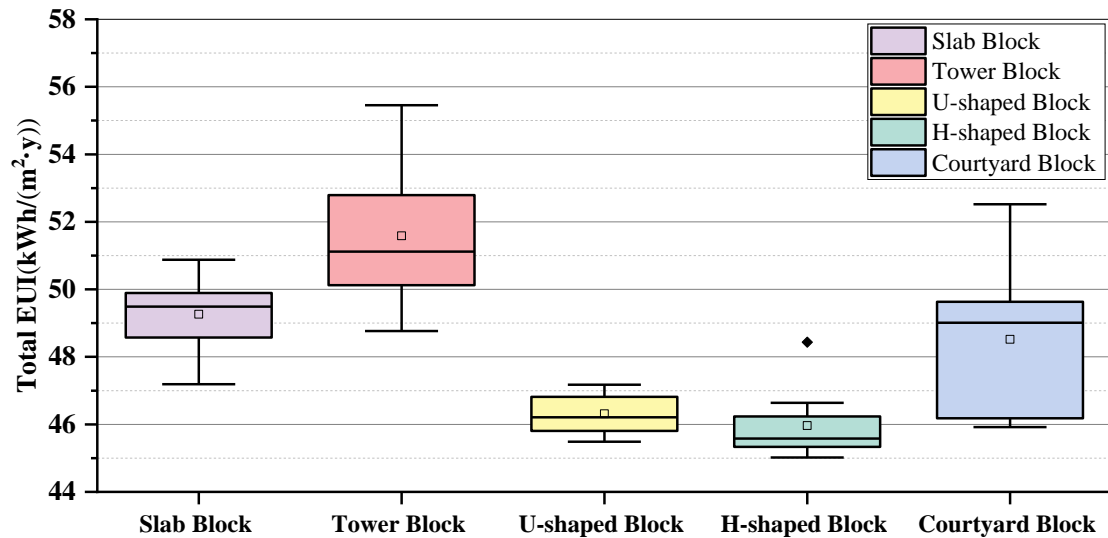


Fig.7. The total EUI by typology

Fig.7 shows distinct variations in the total EUI distribution among the five types. On average, the EUI of the Tower block (51.59 kWh/(m²·y)) was significantly higher than that of the Slab block (49.26 kWh/(m²·y)), followed by the Courtyard block (48.52 kWh/(m²·y)), and U-shaped block (46.32 kWh/(m²·y)), and finally the H-shaped block had the lowest EUI (45.96 kWh/(m²·y)). The maximum and minimum total EUI values differed by 5.63 kWh/(m²·y), indicating a percentage difference of 12.25%. The standard deviation result for the five types was 2.06, suggesting significant differences in total EUI across different block types. EUI results revealed stratified differences among block types, with H-shaped and U-shaped blocks exhibiting higher building energy performance. This highlighted the significance of optimizing block types for achieving optimal building energy performance.

3.3. Solar Energy Generation Intensity

According to Fig. 8, SEGI values were comparable across the rooftops of five block types, whereas significant variations were observed on the facades. The similarity of building heights among dormitory blocks resulted in inadequate rooftop shielding. Conversely, different block types and arrangements led to distinct facade shielding levels and significant SEGI variations.

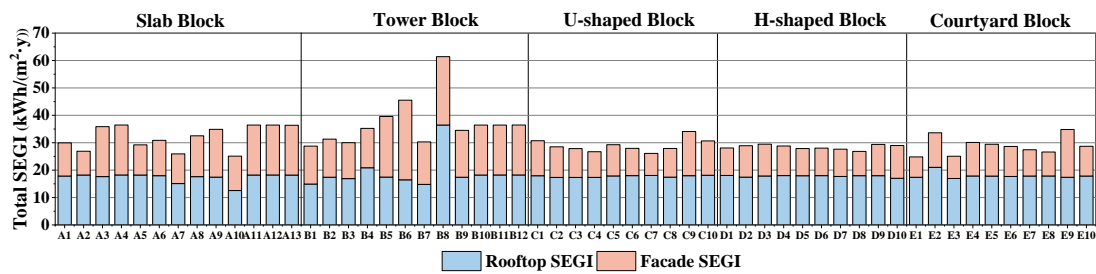


Fig. 8. The total SEGI of 55 blocks

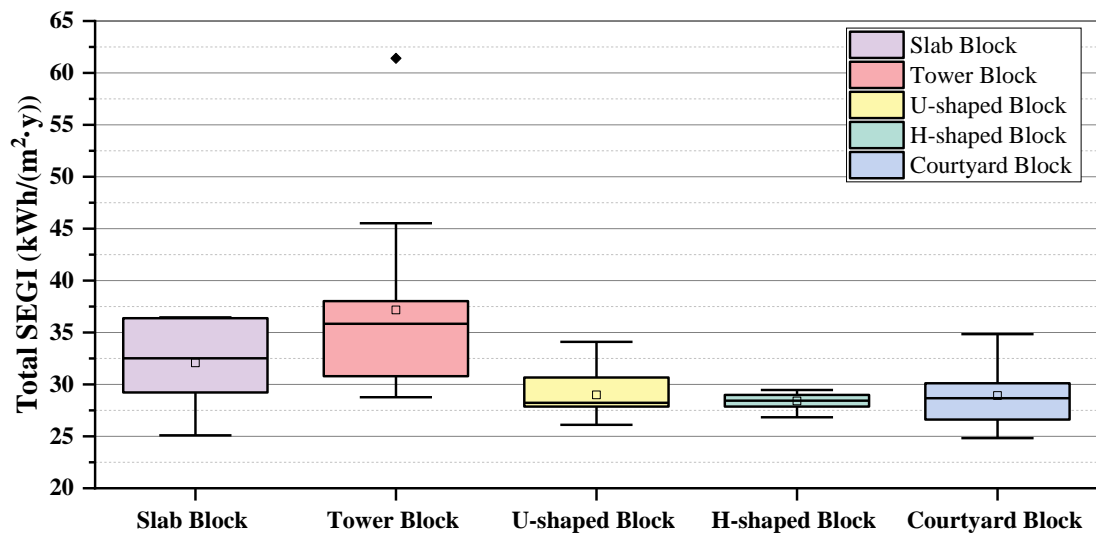


Fig. 9. The total SEGI by typology

Out of the 55 cases, Tower block B8 stood out as a prominent outlier with significantly higher rooftop and facade SEGI values of 36.46 kWh/(m²·y) and 24.95 kWh/(m²·y), respectively. It should be noted that B8 was a three-story dormitory in contrast to the typical six-story ones considered in this study. Since SEGI was measured

per unit building floor area, a roof of the same size would yield vastly different results for buildings of 6 and 3 floors.

Fig. 9 indicates that Tower and Slab blocks had significantly higher mean values of SEGI at 37.17 kWh/(m²·y) and 32.08 kWh/(m²·y), respectively, in comparison to U-shaped (28.98 kWh/(m²·y)), Courtyard (28.93 kWh/(m²·y)), and H-shaped (28.40 kWh/(m²·y)) blocks. The difference in solar energy generation potential between the highest Tower block and the lowest H-shaped block was 8.77 kWh/(m²·y), representing a percentage difference of 30.88%. The standard deviation amongst the five types was 3.30, indicating significant differences in total SEGI among them. However, the SEGI values of U-shaped, H-shaped, and Courtyard blocks were very similar, likely due to the self-shielding effect in the absence of mandatory distance regulations between buildings. Conversely, Tower and Slab blocks maintained certain distances from each other to comply with regulations, resulting in weaker mutual shading effects. The SEGI results revealed that Tower and Slab blocks had substantially greater solar potential than the three enclosed block types (H-shaped, U-shaped and Courtyard blocks). This underlined the importance of optimizing block types to enhance solar energy generation potential.

3.4. Net Energy Use Intensity

As shown in Fig.10 and Fig.11, compared to the H-shaped, U-shaped and Courtyard block, the Tower blocks exhibited a greater fluctuation range in NEUI. With the deployment of PV panels, the order of NEUI from large to small was Courtyard block (19.59 kWh/(m²·y)) > H-shaped block (17.57 kWh/(m²·y)) > U-shaped block

(17.34 kWh/(m²·y)) > Slab block (17.19 kWh/(m²·y)) > Tower block (14.42 kWh/(m²·y)). In Fig. 10, the Y-axis exhibited negative values (-10). It was found that after the deployment of solar panels in case B8, the NEUI became negative, indicating that the solar energy generation potential exceeded the energy use for the block buildings. The Tower block exhibited the most significant improvement in energy performance, with the lowest NEUI value after the deployment of PV panels. The distinct characteristics of the five block types in terms of NEUI further emphasized the importance of integrating building energy consumption with solar energy potential.

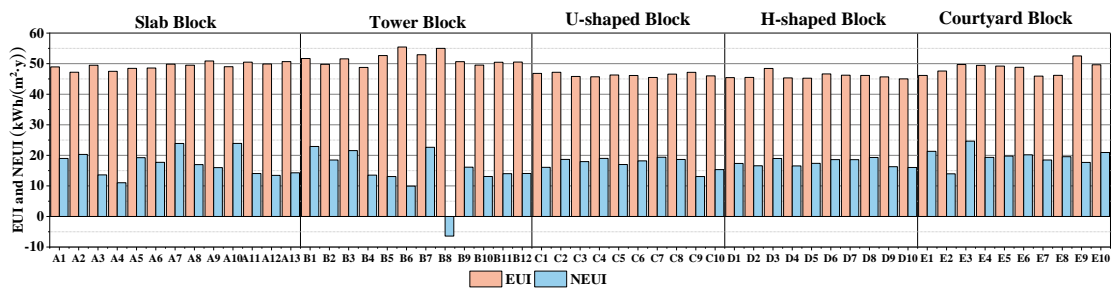


Fig.10. The EUI and NEUI for 55 blocks

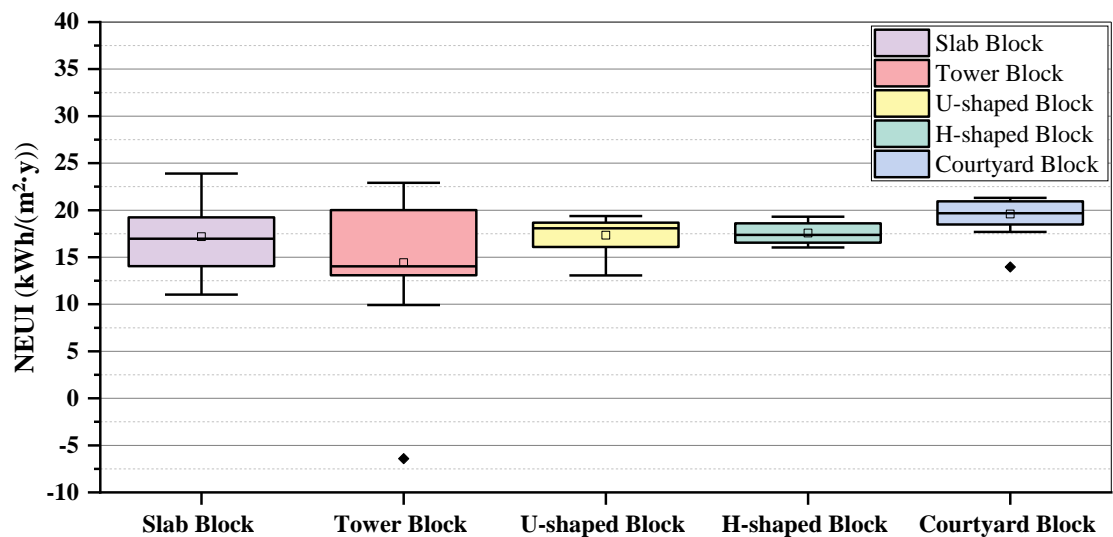


Fig. 11. The total NEUI by typology

4. Discussion

This section first discussed the impact of block typology on three energy performance indicators: EUI, SEGI and NEUI. To further analyze the reasons for the impact, the following discussion analyzed the relationship between urban morphology and the above three energy performance indicators.

4.1. Impact of block typology on building energy performance

The research analyzed 55 dormitory blocks and found that the potential for energy savings at the block level was substantial. The difference in cooling EUI varied by up to 35.58% among different blocks, while the difference in heating EUI was even greater, up to 192.4%. The results show that the impact of urban morphology on heating energy consumption was greater than that of cooling, resulting in a higher variance in heating load than cooling load. This aligns with the findings of previous studies, such as Martins et al. (2019), who reported that height affected the cooling demand by between 7.3% and 8.6%, but that heating demand was affected between 13.6% and 31.2%.

The average EUI values for the highest (Tower) and lowest (H-shaped) block types differed by up to 12.25%. The order of average EUI value of the five blocks from greatest to smallest was Tower block > Slab block > Courtyard block > U-shaped block > H-shaped block. Zhang et al. (2019) found this same phenomenon where the EUI values of Tower blocks and Slab blocks were higher than those of Courtyard blocks in the urban context of Singapore. Compared to other block types, Tower blocks exhibited lower building density, weaker inter-building shading effect, and higher cooling energy consumption in summer. Not only that, they also had the highest SF among all blocks,

which means that heat exchange between buildings and the outdoor environment is facilitated, resulting in the highest EUI.

Compared to EUI, the impact of block typology on NEUI exhibited greater complexity. Specifically, the Tower and Slab blocks demonstrated the highest EUI, whereas the Tower block equipped with PV panels exhibited the lowest NEUI. This observation suggests that the Tower block garnered the most substantial gains from solar energy generation. The deployment of PV panels in dormitory blocks led to an average reduction of 65.0% in EUI. This result was consistent with a study conducted by Hachem-Vermette et al. (2019) on a mixed-use community in Canada, which found that energy generated by PV panels can replace about 70% of a community's total energy use.

As seen in Fig. 9, the Tower block had more variability in the cases compared to the other block types. The possible reasons are as follows. Firstly, the layout of Tower blocks is characterized by a greater degree of variability, with a wider range of dislocated arrangements compared to other block types. Secondly, the height of Tower blocks spans a range of 9 to 21 meters, and this variability has a significant impact on the potential solar power availability per unit building floor area. Finally, the variability of the SF contributes to the variability of heat exchange between Tower blocks and the external environment. Notably, B8, which deviates from the typical pattern of five to six floors observed in other blocks, consists of merely three floors. Of significance was its negative NEUI value, indicating that the 3-story dormitory block generates more solar energy than its energy consumption. These findings suggest that dormitory blocks

with three or four floors have considerable potential for achieving net-zero energy consumption.

4.2. Impact of urban morphology on building energy performance

4.2.1. Correlation analysis between morphological parameters and energy performance indicators

Table 9 presents the correlation between 8 morphological parameters and EUI, SEGI, and NEUI. The parameters that exhibited the strongest correlation with EUI were ALB and SF, with respective correlations of -0.72 and 0.72. BD, FAR, and SVF followed with correlations of 0.71, -0.69, and 0.50, respectively. In a study conducted by Leng et al. (2020) on building heating energy consumption in cold regions of China, BD and FAR were identified as the most relevant indicators affecting energy consumption, consistent with the findings of this study. Furthermore, the results indicate that the effects of BD and FAR on building energy consumption are consistent across different climate regions in China.

Table 9

Results of correlation analysis

Morphological parameters		EUI	SEGI	NEUI
Average length of block (ALB)	Pearson correlation coefficient	-0.72**	-0.46**	0.19
	sig.	0.00	0.00	0.17
Average depth of block (ADB)	Pearson correlation coefficient	-0.23	-0.15	0.07
	sig.	0.09	0.27	0.63
Average height of block (AHB)	Pearson correlation coefficient	-0.13	-0.63**	0.74**
	sig.	0.33	0.00	0.00
Sky View factor (SVF)	Pearson correlation coefficient	0.50**	0.64**	-0.55**
	sig.	0.00	0.00	0.00
Shape factor (SF)	Pearson correlation coefficient	0.72**	0.78**	-0.60**
	sig.	0.00	0.00	0.00

Height to depth ratio (HDR)	Pearson correlation coefficient	0.15	-0.13	0.25
	sig.	0.26	0.35	0.07
Building density (BD)	Pearson correlation coefficient	-0.71**	-0.56**	0.32*
	sig.	0.00	0.00	0.02
Floor area ratio (FAR)	Pearson correlation coefficient	-0.69**	-0.71**	0.53**
	sig.	0.00	0.00	0.00

** means the correlation was significant at level 0.01.
* means the correlation was significant at level 0.05.

	ALB	ADB	AHB	SVF	SF	HDR	BD	FAR	EUI	SEGI	NEUI	
ALB	1.00	-0.03	0.20	-0.56	-0.57	0.06	0.57	0.59	-0.72	-0.46	0.20	ALB
ADB	-0.03	1.00	0.00	-0.07	-0.53	-0.86	0.30	0.26	-0.23	-0.15	0.07	ADB
AHB	0.20	0.00	1.00	-0.33	-0.48	0.37	0.06	0.40	-0.13	-0.63	0.74	AHB
SVF	-0.56	-0.07	-0.33	1.00	0.53	-0.06	-0.65	-0.71	0.50	0.64	-0.55	SVF
SF	-0.57	-0.53	-0.48	0.53	1.00	0.32	-0.67	-0.76	0.72	0.78	-0.60	SF
HDR	0.06	-0.86	0.37	-0.06	0.32	1.00	-0.26	-0.11	0.15	-0.13	0.25	HDR
BD	0.57	0.30	0.06	-0.65	-0.67	-0.26	1.00	0.93	-0.71	-0.56	0.32	BD
FAR	0.59	0.26	0.40	-0.71	-0.76	-0.11	0.93	1.00	-0.69	-0.71	0.53	FAR
EUI	-0.72	-0.23	-0.13	0.50	0.73	0.15	-0.71	-0.69	1.00	0.68	-0.32	EUI
SEGI	-0.46	-0.15	-0.63	0.64	0.78	-0.13	-0.56	-0.71	0.68	1.00	-0.91	SEGI
NEUI	0.20	0.07	0.74	-0.55	-0.60	0.25	0.32	0.53	-0.32	-0.91	1.00	NEUI
	ALB	ADB	AHB	SVF	SF	HDR	BD	FAR	EUI	SEGI	NEUI	
	-1.00	-0.75	-0.50	-0.25	-0.15	0.00	0.15	0.25	0.50	0.75	1.00	
	Negative correlation($p > -0.05$)					Irrelevant($p > 0.05$)			Positive correlation($p < 0.05$)			

Fig. 12. Heat map of correlation results

Based on the findings presented in Fig.12, the SF exhibited the most significant impact on both EUI and SEGI, while also emerging as one of the key morphological parameters affecting NEUI. These results highlight the importance of controlling SF when designing low-energy dormitory blocks on campus. Specifically, SF serves as a

critical determinant of the building surface area, which plays a crucial role in mediating energy exchange between the exterior environment and interior spaces, as well as serving as a platform for the installation of solar PV panels.

Building height exhibited a weak correlation with EUI and a strong correlation with SEGI. There are two factors contributing to the negative correlation between AHB and SEGI. Firstly, an increase in building height results in greater mutual occlusion between buildings. Secondly, as the unit of SEGI for the current study was defined as per unit building floor area, an increase in building height leads to a larger total building floor area without a corresponding increase in the main installation areas for solar PV panels, such as rooftops. According to previous studies (Zhang et al., 2019; Xia et al., 2021), the SEGI was found to be more susceptible to the impact of urban morphology than the EUI, resulting in the emergence of AHB as one of the most significant parameters affecting the NEUI.

The correlation between the morphological parameters and energy performance indicators varied, and different indicators should be considered for block-scale planning proposals. Liu et al. (2023) suggest that residential neighborhoods in Hot-summer and Cold-winter zone should have a floor area ratio of 1.5 for development intensity control, based on energy use and solar energy potential considerations. Energy efficiency campus planning in Wuhan, which shares the same climate zone, should adjust parameters according to specific building performance requirements.

4.2.2. Multiple linear regression model to predict building energy performance

The correlation between individual morphological parameters and energy

performance indicators was calculated using a correlation analysis. However, this method could not fully explain the combined influence of morphological parameters on the energy performance results. To address this, this study conducted a multiple regression analysis by selecting morphological parameters with strong correlation based on the correlation analysis. The backward selection method was employed in this study. Although multiple models can be generated by multiple regression analysis, only the morphological parameters retained in the final model that passed the correlation test were considered significant.

Table 10

Results of multiple regression analysis

Regression model		Unstandardized coefficients		Standardized coefficients	Sig.	Collinear statistics	Adjusted R ²
Dependent variable	Independent Variable	B	standard error	Beta		VIF	
EUI	(Constant)	50.71	2.48	-	-	-	0.69
	ALB	-0.05	0.01	-0.38	0.00	1.64	
	SF	19.36	6.57	0.32	0.01	1.99	
	BD	-10.72	3.95	-0.29	0.01	1.98	
SEGI	(Constant)	20.75	7.56	-	-	-	0.73
	SF	68.18	12.71	0.48	0.00	1.62	
	SVF	0.28	0.08	0.29	0.00	1.40	
	AHB	-1.07	0.28	-0.31	0.00	1.31	
NEUI	(Constant)	5.11	6.71	-	-	-	0.65
	AHB	1.52	0.25	0.56	0.00	1.31	
	SVF	-0.20	0.07	-0.26	0.01	1.40	
	SF	-21.59	11.28	-0.20	0.06	1.62	

Table 10 displays the adjusted R² values of the final regression models of EUI, SEGI and NEUI were 0.69, 0.73 and 0.65, respectively, all of which had a good degree of fit and statistical significance. The EUI was primarily affected by three

morphological parameters, which were ranked according to their degree of influence (standardized Beta value): ALB (-0.38) had the most significant effect, followed by SF (0.32), and then BD (-0.29). The EUI can be calculated by Eq. (6).

$$EUI = 50.71 - 0.05 \times ALB + 19.36 \times SF - 10.72 \times BD \quad (6)$$

According to the results of multiple regression, for the all blocks, the ALB, SF and BD had the most significant impact on the total EUI. ALB and BD were found to have a negative correlation with EUI. Specifically, with an increase in ALB of 1 unit, building EUI decreased by 0.05 kWh/(m²·y), and with an increase in BD of 0.1 units, building EUI decreased by 1.07 kWh/(m²·y). On the other hand, SF was positively correlated with EUI, and an increase in SF of 0.1 units resulted in an increase in building EUI by 1.94 kWh/(m²·y).

Three morphological parameters significantly impacted the SEGI, ranked by their standardized Beta values: SF (0.48) had most significant effect, followed by AHB (-0.31) and SVF (0.29). Through the backward selection method, 5 multiple models were generated, with the final regression model of SEGI achieving a high degree of fit and statistical significance, as evidenced by an adjusted R² value of 0.64. SEGI can be calculated by Eq. (7).

$$SEGI = 20.75 + 68.18 \times SF - 1.07 \times AHB + 0.28 \times SVF \quad (7)$$

Results from multiple regression showed that SF and AHB had the greatest impact on total SEGI for all blocks. AHB had a negative correlation with SEGI, with each unit increase resulting in a 1.07 kWh/(m²·y) decrease. On the other hand, SF and SVF had a significant positive correlation with SEGI, with an increase of 6.82 kWh/(m²·y) in

SEGI for each 0.1 unit increase in SF, and an increase of 0.28 kWh/(m²·y) in SEGI for each unit increase in SVF.

Three morphological parameters significantly impacted the NEUI values, with their influence ranked by their standardized Beta values. The AHB exhibited the strongest effect (0.56), followed by the SF (-0.26) and SVF (-0.20). NEUI can be calculated by Eq. (8).

$$NEUI = 5.11 + 1.52 \times AHB - 21.59 \times SF - 0.20 \times SVF \quad (8)$$

Multiple regression results showed that the SF and AHB had the most significant impact on NEUI. The AHB had a positive correlation with NEUI, with each unit increase resulting in a 1.52 kWh/(m²·y) increase. The SF and SVF had negative correlations with NEUI, with a 0.1 unit increase in SF leading to a 2.16 kWh/(m²·y) decrease, and each unit increase in SVF resulting in a 0.20 kWh/(m²·y) decrease.

This study provided compelling evidence for the impact of urban morphology on building energy performance indicators such as EUI, SEGI, and NEUI, which exhibit significant differences between EUI and NEUI due to the varying degree of influence of urban morphology. Xia et al. (2021) reported comparable results in their investigation on optimizing building energy consumption and solar potential in residential blocks in Hot-summer and Cold-winter zone in China. The research demonstrated that solar radiation access was more sensitive to the urban morphology variation than energy consumption. Furthermore, the morphological parameters, including FAR and BD, exerted significant but distinct effects on performance indicators. The findings demonstrate that the SF is a crucial influencing factor for all

three performance indicators. Furthermore, solar potential is more sensitive to the urban morphology variation than energy consumption. To minimize NEUI, parameter adjustments are required to maximize SEGI. Finally, dormitory blocks may require tailored urban morphology to optimize building energy performance with or without the deployment of PV panels.

4.3. Limitations

This study primarily examined the impact of urban morphology on building energy consumption and solar energy potential. Building energy consumption is a multifactorial phenomenon that is influenced by a range of factors, such as building envelope, construction materials, occupancy, and equipment load. To evaluate the impact of urban morphology on building energy intensity, these variables must be simplified and standardized to assess the singular influence of a variable on energy consumption. Future research can aim to refine the types of research subjects further to compensate for the imprecision that arises from simplification.

5. Conclusion

This study examined the impact of urban morphology on building energy consumption and solar energy generation potential in university dormitory blocks located in the Hot-summer and Cold-winter zone in China. Five block types were classified, and Ladybug and Honeybee simulation tools were used to calculate EUI and SEGI. The impact of eight urban morphological parameters on EUI, SEGI, and NEUI were evaluated. The findings provided compelling evidence that block topology and urban morphology significantly impact energy consumption and solar energy

generation potential at the block-scale. According to studies it was found that:

- (1) Block typologies result in significant differences in building EUI, SEGI and NEUI of up to 12.25%, 30.88% and 35.85%, respectively.
- (2) H-shaped and U-shaped blocks exhibit better EUI performance than other types, while Tower blocks benefit the most from PV deployment, surpassing other types with the lowest NEUI.
- (3) SEGI is more sensitive to the urban morphological variation than EUI.
- (4) The primary morphological parameters that affect EUI are ALB, SF, and BD, while SEGI and NEUI are primarily influenced by SF, AHB, and SVF.
- (5) The proposed multiple linear regression models can effectively predict EUI, SEGI, and NEUI, with a fitting degree of 0.69, 0.73, and 0.65, respectively.

The results of this study could serve as guidelines for planners and policy makers in campus energy planning and architectural design to improve building energy conservation and clean energy policy development at the block-scale. The technical framework developed in this study can facilitate effective decision-making, especially in conducting feasibility studies in the early stages of campus planning and building design. It can be applied to other cities and climate regions to evaluate building energy consumption and solar energy generation potential at block-scale, to determine the most efficient planning and design solutions suitable for the local environment.

Funding

1. Supported by program for HUST Academic Frontier Youth Team

(No.2019QYTD10) and Fundamental Research Funds for the Central Universities
(No.2019kfyXKJC029)

2. National Natural Science Foundation (No. 51678261; 51978296)
3. Project 1520104: Assessing The Impact Of Built Form And Vegetation Metric On Energy Consumption: Pilot Project On University Campus Optimizing Design.
Newton Fund Grant Researcher Links Workshop 2021 2020-RLWK12-10633

Appendix 1 Investigated Personnel Information

Gender	Male (51%), Female (49%)
Academic degree	Associate's (12%), Bachelor's (63%), Master's (21%), Doctoral (4%)

Appendix 2 Content of survey questionnaires

Table A1

Survey Questionnaire Information

Building information	Year of construction, number of rooms per unit, layout, building type
Type of energy-using equipment	Cooling: fans, local air conditioner unit, central air conditioning Heating: electric heating, local air conditioner unit, centralized heating
energy use Information	Energy use intensity, energy consumption time
human behavior Information	Number of days per year indoors, weekday vs weekend occupancy, time spent indoors per day

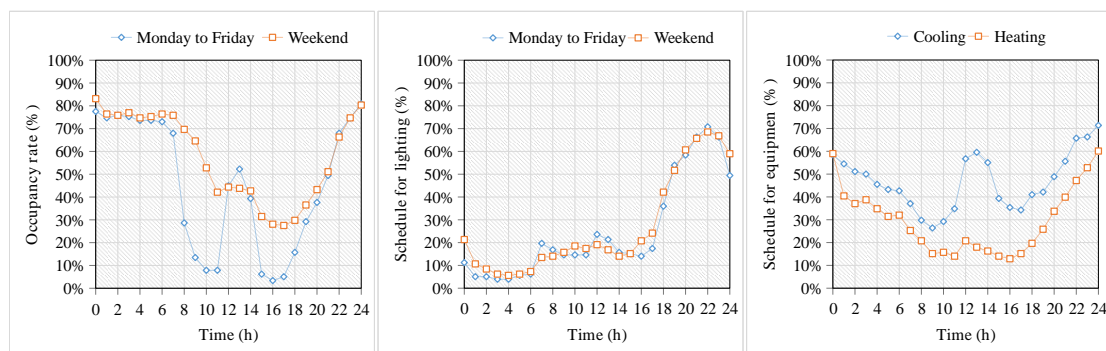


Fig.A1. The investigation result of schedule.

References

- Ahmadian, E., Sodagar, B., Bingham, C., Elnokaly, A., & Mills, G. (2021). Effect of urban built form and density on building energy performance in temperate climates. *Energy and Buildings*, 236, 110762.
<https://doi.org/10.1016/j.enbuild.2021.110762>
- Amaral, A. R., Rodrigues, E., Rodrigues Gaspar, A., & Gomes, Á. (2018). Review on performance aspects of nearly zero-energy districts. *Sustainable Cities and Society*, 43(June), 406–420. <https://doi.org/10.1016/j.scs.2018.08.039>
- Bansal, P., & Jige, S. (2022). Energy & Buildings Relationships between building characteristics , urban form and building energy use in different local climate zone contexts : An empirical study in Seoul. *Energy & Buildings*, 272, 112335.
<https://doi.org/10.1016/j.enbuild.2022.112335>
- Bland, Martin (2015). *An Introduction to Medical Statistics*. Fourth ed. Oxford UP. Oxford Medical Publications.
- Chen, Z., Yu, B., Li, Y., Wu, Q., Wu, B., Huang, Y., Wu, S., Yu, S., Mao, W., Zhao, F., & Wu, J. (2022). Assessing the potential and utilization of solar energy at the building-scale in Shanghai. *Sustainable Cities and Society*, 82, 103917.
<https://doi.org/10.1016/j.scs.2022.103917>
- Fan, Z., Xiao, Z., & Liu, J. (2022). Energy performance assessment of semi-transparent photovoltaic integrated large-scale railway stations among various climates of China. *Energy Conversion and Management*, 269, 115984.
<https://doi.org/10.1016/j.enconman.2022.115984>

-
- Hachem-Vermette, C., Guarino, F., La Rocca, V., & Cellura, M. (2019). Towards achieving net-zero energy communities: Investigation of design strategies and seasonal solar collection and storage net-zero. *Solar Energy*, 192(July 2018), 169–185. <https://doi.org/10.1016/j.solener.2018.07.024>
- Huang, Z., Mendis, T., & Xu, S. (2019). Urban solar utilization potential mapping via deep learning technology: A case study of Wuhan, China. *Applied Energy*, 250, 283–291. <https://doi.org/10.1016/j.apenergy.2019.04.113>
- Iturriaga, E., Campos-Celador, Á., Terés-Zubiaga, J., Aldasoro, U., & Álvarez-Sanz, M. (2021). A MILP optimization method for energy renovation of residential urban areas: Towards Zero Energy Districts. *Sustainable Cities and Society*, 68. <https://doi.org/10.1016/j.scs.2021.102787>
- Izquierdo, S., Rodrigues, M., & Fueyo, N. (2008). A method for estimating the geographical distribution of the available roof surface area for large-scale PV energy-potential evaluations. *Solar Energy*, 82(10), 929–939. <https://doi.org/10.1016/j.solener.2008.03.007>
- Lan, H., Gou, Z., & Xie, X. (2021). A simplified evaluation method of rooftop solar energy potential based on image semantic segmentation of urban streetscapes. *Solar Energy*, 230, 912–924. <https://doi.org/10.1016/j.solener.2021.10.085>
- Leng, H., Chen, X., Ma, Y., Wong, N. H., & Ming, T. (2020). Urban morphology and building heating energy consumption: Evidence from Harbin, a severe cold region city. *Energy and Buildings*, 224, 110143. <https://doi.org/10.1016/j.enbuild.2020.110143>

-
- Liu, K., Xu, X., Zhang, R., Kong, L., Wang, W., & Deng, W. (2023). Energy & Buildings Impact of urban form on building energy consumption and solar energy potential: A case study of residential blocks in Jianhu, China. *Energy & Buildings*, 280, 112727. <https://doi.org/10.1016/j.enbuild.2022.112727>
- Liao, W., Heo, Y., & Xu, S. (2019). Simplified vector-based model tailored for urban-scale prediction of solar irradiance. *Solar Energy*, 183(August 2018), 566–586. <https://doi.org/10.1016/j.solener.2019.03.023>
- Martins, T. A. de L., Faraut, S., & Adolphe, L. (2019). Influence of context-sensitive urban and architectural design factors on the energy demand of buildings in Toulouse, France. *Energy and Buildings*, 190, 262–278. <https://doi.org/10.1016/j.enbuild.2019.02.019>
- Mendis, T., Huang, Z., Xu, S., & Zhang, W. (2020). Economic potential analysis of photovoltaic integrated shading strategies on commercial building facades in urban blocks: A case study of Colombo, Sri Lanka. *Energy*, 194, 116908. <https://doi.org/10.1016/j.energy.2020.116908>
- Oh, M., & Kim, Y. (2019). Identifying urban geometric types as energy performance patterns. *Energy for Sustainable Development*, 48, 115–129. <https://doi.org/10.1016/j.esd.2018.12.002>
- Poon, K. H., Kämpf, J. H., Tay, S. E. R., Wong, N. H., & Reindl, T. G. (2020). Parametric study of URBAN morphology on building solar energy potential in Singapore context. *Urban Climate*, 33, 100624. <https://doi.org/10.1016/j.uclim.2020.100624>

-
- Prataviera, E., Vivian, J., Lombardo, G., & Zarrella, A. (2022). Evaluation of the impact of input uncertainty on urban building energy simulations using uncertainty and sensitivity analysis. *Applied Energy*, 311(January).
<https://doi.org/10.1016/j.apenergy.2022.118691>
- Quan, S. J., & Li, C. (2021). Urban form and building energy use: A systematic review of measures, mechanisms, and methodologies. *Renewable and Sustainable Energy Reviews*, 139(December 2020), 110662.
<https://doi.org/10.1016/j.rser.2020.110662>
- Ren, H., Xu, C., Ma, Z., & Sun, Y. (2022). A novel 3D-geographic information system and deep learning integrated approach for high-accuracy building rooftop solar energy potential characterization of high-density cities. *Applied Energy*, 306(PA), 117985. <https://doi.org/10.1016/j.apenergy.2021.117985>
- Sarralde, J. J., Quinn, D. J., Wiesmann, D., & Steemers, K. (2015). Solar energy and urban morphology: Scenarios for increasing the renewable energy potential of neighbourhoods in London. *Renewable Energy*, 73, 10–17.
<https://doi.org/10.1016/j.renene.2014.06.028>
- Shi, Y., Yan, Z., Li, C., & Li, C. (2021). Energy consumption and building layouts of public hospital buildings: A survey of 30 buildings in the cold region of China. *Sustainable Cities and Society*, 74, 103247.
<https://doi.org/10.1016/j.scs.2021.103247>
- Suh, H. S., & Kim, D. D. (2019). Energy performance assessment towards nearly zero energy community buildings in South Korea. *Sustainable Cities and Society*,

44(October 2018), 488–498. <https://doi.org/10.1016/j.scs.2018.10.036>

Ullah, K. R., Prodanovic, V., Pignatta, G., Deletic, A., & Santamouris, M. (2021).

Technological advancements towards the net-zero energy communities: A review on 23 case studies around the globe. *Solar Energy*, 224(May), 1107–1126.

<https://doi.org/10.1016/j.solener.2021.06.056>

UN-Habitat, energy, 2021(accessed on 16 July,2022)

<https://unhabitat.org/topic/energy>

Wang, P., Liu, Z., & Zhang, L. (2021). Sustainability of compact cities: A review of

Inter-Building Effect on building energy and solar energy use. *Sustainable Cities and Society*, 72, 103035. <https://doi.org/10.1016/j.scs.2021.103035>

Xia, B., & Li, Z. (2021). Optimized methods for morphological design of mesoscale

cities based on performance analysis: Taking the residential urban blocks as examples. *Sustainable Cities and Society*, 64(March 2020), 102489.

<https://doi.org/10.1016/j.scs.2020.102489>

Xu, S., Huang, Z., Wang, J., Mendis, T., & Huang, J. (2019). Evaluation of PV

potential by urban block typology: A case study of Wuhan, China. *Renewable Energy Focus*, 29(June), 141–147. <https://doi.org/10.1016/j.ref.2019.03.002>

Xu, S., Jiang, H., Xiong, F., Zhang, C., Xie, M., & Li, Z. (2021). Evaluation for

block-scale solar energy potential of industrial block and optimization of

application strategies : A case study of Wuhan , China. *Sustainable Cities and Society*, 72(May), 103000. <https://doi.org/10.1016/j.scs.2021.103000>

Zhang, J., Xu, L., Shabunko, V., Tay, S. E. R., Sun, H., Lau, S. S. Y., & Reindl, T.

(2019). Impact of urban block typology on building solar potential and energy use efficiency in tropical high-density city. *Applied Energy*, 240(August 2018), 513–533. <https://doi.org/10.1016/j.apenergy.2019.02.033>